



AFRL-OSR-VA-TR-2013-0530

**BUCKLING OF BILAYER LAMINATES - A NOVEL APPROACH TO
SYNTHETIC PAPILLAE**

SACHIN VELANKAR

UNIVERSITY OF PITTSBURGH THE

10/01/2013

Final Report

DISTRIBUTION A: Distribution approved for public release.

**AIR FORCE RESEARCH LABORATORY
AF OFFICE OF SCIENTIFIC RESEARCH (AFOSR)/RSL
ARLINGTON, VIRGINIA 22203
AIR FORCE MATERIEL COMMAND**

REPORT DOCUMENTATION PAGE				<i>Form Approved</i> OMB No. 0704-0188	
Public reporting burden for this collection of information is estimated to average 1 hour per response, including the time for reviewing instructions, searching existing data sources, gathering and maintaining the data needed, and completing and reviewing this collection of information. Send comments regarding this burden estimate or any other aspect of this collection of information, including suggestions for reducing this burden to Department of Defense, Washington Headquarters Services, Directorate for Information Operations and Reports (0704-0188), 1215 Jefferson Davis Highway, Suite 1204, Arlington, VA 22202-4302. Respondents should be aware that notwithstanding any other provision of law, no person shall be subject to any penalty for failing to comply with a collection of information if it does not display a currently valid OMB control number. PLEASE DO NOT RETURN YOUR FORM TO THE ABOVE ADDRESS.					
1. REPORT DATE (DD-MM-YYYY) 09/29/2013		2. REPORT TYPE Final technical		3. DATES COVERED (From - To) 07/01/2010-06/30/2013	
4. TITLE AND SUBTITLE Buckling of bilayer laminates- A novel approach to synthetic papillae				5a. CONTRACT NUMBER FA9550-10-1-0329	
				5b. GRANT NUMBER	
				5c. PROGRAM ELEMENT NUMBER	
6. AUTHOR(S) Sachin Velankar, Dept of Chemical Engineering, University of Pittsburgh				5d. PROJECT NUMBER	
				5e. TASK NUMBER	
				5f. WORK UNIT NUMBER	
7. PERFORMING ORGANIZATION NAME(S) AND ADDRESS(ES) University of Pittsburgh, Dept. of Chemical Engineering, 1249 Benedum Hall, Pittsburgh PA 15238				8. PERFORMING ORGANIZATION REPORT NUMBER	
9. SPONSORING / MONITORING AGENCY NAME(S) AND ADDRESS(ES) AFOSR 875 N. Randolph St Arlington, VA 22203				10. SPONSOR/MONITOR'S ACRONYM(S)	
				11. SPONSOR/MONITOR'S REPORT NUMBER(S)	
12. DISTRIBUTION / AVAILABILITY STATEMENT A = Approved for public release; distribution is unlimited					
13. SUPPLEMENTARY NOTES					
14. ABSTRACT Cephalopods can reversibly change their appearance by expressing papillae – folds, bumps, spikes, or even more complex structures – on their skin for camouflage purposes. This project, in collaboration with Dr. Roger Hanlon, Marine Biological Laboratory, sought to examine the biomechanics of papillae formation, develop methods to simulate papillae formation, and develop biomimetic artificial papillae using synthetic materials. We have developed image correlation methods to analyze video of the active skin of cuttlefish, attempted several methods of measuring the skin mechanical properties, and contributed to research on the musculature of papillae. On the simulations side, we have developed a simple method of modulus perturbations for the numerical modeling of elastic instabilities. On the biomimetic side, we have developed a general platform using shape memory alloys that can develop reversible surface texture at the flip of a switch, and detailed mechanical model of the same using a shear lag approach. Finally, we have also examined the buckling of swollen crosslinked films, and buckling of thin films floating on viscous liquids.					
15. SUBJECT TERMS					
16. SECURITY CLASSIFICATION OF:			17. LIMITATION OF ABSTRACT unclassified (U)	18. NUMBER OF PAGES	19a. NAME OF RESPONSIBLE PERSON Sachin Velankar
a. REPORT unclassified	b. ABSTRACT unclassified	c. THIS PAGE unclassified			19b. TELEPHONE NUMBER (include area code) 412-624-9984

Buckling of bilayer laminates- A novel approach to synthetic papillae

Grant/Contract Number: FA9550-10-1-0329

Final report

Abstract

Cephalopods can reversibly change their appearance by expressing papillae – folds, bumps, spikes, or even more complex structures – on their skin for camouflage purposes. This project, in collaboration with Dr. Roger Hanlon, Marine Biological Laboratory, sought to examine the biomechanics of papillae formation, develop methods to simulate papillae formation, and develop biomimetic artificial papillae using synthetic materials. A key hypothesis at the beginning of this project is that some papillae are formed by a skin buckling mechanism where muscular action induces compressive stress on the skin and which then buckles into papillae.

On the biological side, we developed image correlation methods to analyze video of the active skin of cuttlefish *Sepia Officinalis* (videos provided by Hanlon lab) to quantify its mechanics. We find that with neural stimulation, the active skin can compress up to 40% over timescales of roughly 1 second. We also attempted several methods of measuring the skin mechanical properties: inflation, AFM, or indentation at larger lengthscales. While the last was at least partially successful, the fact that the skin is highly active and mobile under measurement conditions is a major obstacle to quantifying the mechanical properties of live skin. Finally, the PI contributed the research in the Hanlon laboratory on deciphering the mechanism of papillae extension by examining the musculature of papillae. Most papillae are erected by a muscular hydrostatic mechanism rather than a skin buckling mechanism (in opposition to the hypothesis made at the beginning of the project). One exception is the face papillae of *S. Apama* which do seem to follow a buckling mechanism.

On the simulations side, we have developed a simple method of modulus perturbations for the numerical modeling of elastic instabilities. We show that this method is able to capture - with quantitative accuracy – a variety of buckling problems, including some which cannot be predicted by linear stability analysis. Further advantages are that the simulation method need not be tailored to individual geometries, that the simulation method can capture post-buckling mode changes, and that the simulation uses commercial simulation software needing no specialized knowledge of stability analysis. Finally, in light of the fact that many papillae are driven by muscular hydrostats, we have developed a simulation method to capture shape changes due to complex muscular arrangements. Specifically, we use thermomechanical calculations built into commercial FEM software (using anisotropic thermal expansion coefficients) to model muscular hydrostats. The advantage is that shape

changes can be estimated by simply knowing muscular arrangements with no further details needed. The disadvantage is that the dynamics or forces involved are not included in the calculations.

On the biomimetic side, we have developed a general platform that can develop reversible surface texture at the flip of a switch. It uses shape memory alloy wires embedded in an elastomer to induce surface compression, which is in turn used to drive buckling of the surface. The platform can reversibly go from being smooth to textured within few second timescales with low voltage ($< 10V$) actuation analogous to cuttlefish skin. We have also developed a detailed mechanical model of the same using shear lag theory to provide design tools for reversibly-texturing surfaces.

Finally we have made progress in two projects that were not directly related to cephalopods, but nevertheless relevant to texture formation: the swelling and folding of crosslinked polymer films attached to surfaces, and buckling of thin films with viscous supports.

Cephalopods can reversibly change their appearance by expressing papillae – folds, bumps, spikes, or even more complex structures – on their skin. This allows the animals to camouflage themselves by changing the outline of their own bodies and by mimicking the texture of the surroundings[1, 2]. This research sought to elucidate the biomechanics of the expression of papillae, and to replicate similar skin-texturing ability in synthetic systems. The biological portion of this research was conducted collaboratively with the laboratory of Dr. Roger Hanlon, Marine Biological Laboratory, Woods Hole, MA.

The publications have taken longer than expected: some articles have been submitted, whereas some are still in progress. We anticipate the following articles to result from this funding:

1. S.S. Velankar, V. Lai, R.A. Vaia, “Swelling-induced delamination causes folding of surface-tethered polymer gels”, *ACS App. Mat. Int.*, **4**, 24-29, 2012.
2. J.J. Allen, G.R.R. Bell, A.M. Kuzirian, S.S. Velankar, R. T. Hanlon “Comparative morphology of changeable skin papillae in octopus and cuttlefish”, in revision, *Journal of Morphology*.
3. Derek Breid, Victoria Lai, Andrew T. Flowers, Sachin S. Velankar, Modes of folding during swelling-induced delamination of crosslinked polymer films”, submitted to *European Physical Journal E*.
4. S. Chatterjee and S.S. Velankar, “SMA-elastomer composites for reversibly-morphing surfaces” to be submitted to *Journal of Intelligent Material Systems and Structures* (submission expected October 2013).
5. R. A. Wulandana and S.S. Velankar, “Random modulus perturbation method for direct numerical simulations of elastic instabilities”, to be submitted to *Computers and Structures* (submission expected October 2013)
6. S. Chatterjee, R. Huang and S.S. Velankar, “Compression-induced buckling of elastic films on viscous substrates. Part 1: Shear lag model”, to be submitted.
7. S. Chatterjee, C.L. McDonald J. Niu and S.S. Velankar, “Compression-induced buckling of elastic films on viscous substrates. Part 2: Experimental”, to be submitted.
8. P. Golzalez, P., S. Chatterjee, S.S. Velankar, R.T. Hanlon, “Mechanics of active skin in *Sepia Officinalis*”, to be submitted.

In the following, we will discuss the activities undertaken and the results of this research. The report will especially document results or activities that will **not** be reflected in the publications, and hence will not be on archive elsewhere.

Video tracking of active skin mechanics

We have developed video analysis methods for quantitative analysis of skin displacement measurements of the active skin. The chief goal of this analysis was to answer the following questions (1) how much strain does the active skin undergo due to gross motion (i.e. motion not specifically linked to papillae), (2) is the strain uniform across the entire skin, or heterogeneous, and (3) what are the timescales of papillae formation.

Video analysis of active skin is significantly more complicated than in applications such as particle tracking velocimetry because the appearance of skin can change significantly, both locally (individual chromatophores expand and contract) and on an average (an entire region of skin can appear darker because numerous chromatophores expanded). An example of video analysis is shown in Fig. 1. It shows two frames of cuttlefish (*S. officinalis*) skin undergoing neural excitation. These experiments were conducted by Dr. Paloma Gonzalez at the Marine Biological Laboratory. Papillae were not raised during this excitation, but the skin underwent gross area changes. However there was also significant local darkening of the skin, which makes video analysis more challenging. Nevertheless our digital image correlation (DIC) code can follow the skin deformation, as illustrated by the deformed grid in Fig. 1B.

From such DIC analysis, the strain in the skin can be calculated. Fig. 1C illustrates the strain map in the region of interest which is essentially a measure of the local area changes occurring between Fig. 1A and Fig. 1B. By conducting such strain analysis across the entire sequence of video frames, the evolution of skin strain under neural stimulation can be obtained. The rise in strain is nearly exponential and can be well-fitted by

$$\epsilon = \epsilon_0 \exp\left(-\frac{t}{\tau}\right)$$

where τ is the time constant characteristic of the excitation. These time constants are illustrated in Fig. 1E. We conclude that higher neural excitation frequency leads to faster excitation. We have also examined histograms of the strain maps (i.e. the frequency with which a given area change appears) and typically the largest strains encountered are roughly 40% changes in area. The magnitude of these area changes far exceeds the capabilities of synthetic smart surfaces. Moreover the fact that such compression is not accompanied by buckling suggests that either the skin does not have a significant modulus heterogeneity in the thickness direction, or that it is under significant pre-tension. This is the first quantification of area changes of the cuttlefish active skin. Finally we note that in any given animal, experiments examined excitation of different nerves, and there are significant differences in the area changes and the time scales of excitation between nerves. These results are a part of a publication by Dr. Gonzalez, presently in progress.

A key unresolved issue is quantifying the dynamics of papillae formation and lowering, and in particular comparing their timescales. This requires 3D image correlation, which in turn requires two-camera monitoring of the active skin.

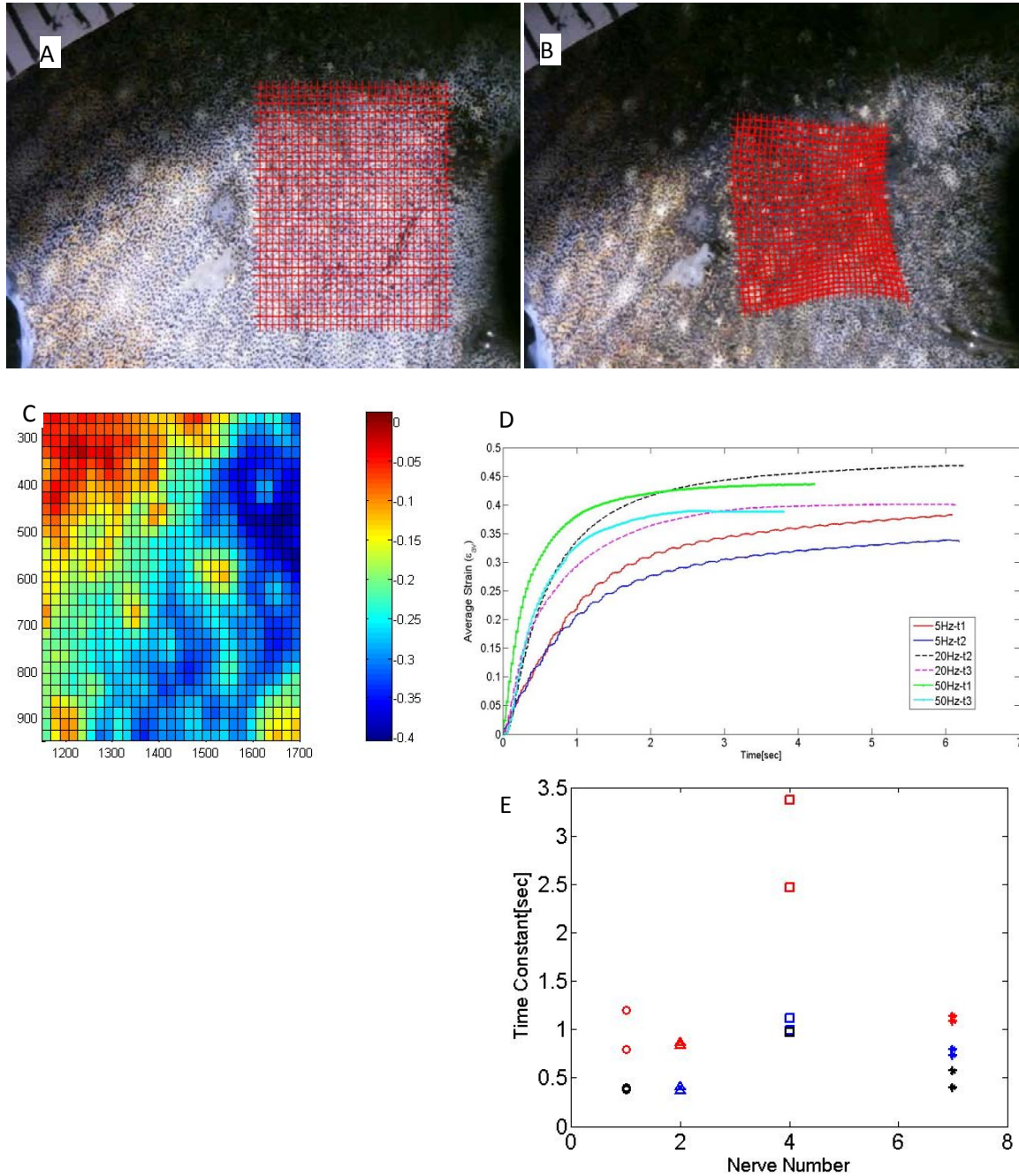


Figure 1: A&B: Video images of skin under neural excitation. Frames extracted from video provided by Dr. Paloma Gonzalez from the laboratory of Dr. Roger Hanlon. The grid is used to track the deformation of the skin. **C.** The compressional strain map of the skin. **D.** The kinetics of skin contraction in experiments at different neural excitation frequencies where red symbols are 5 Hz excitation, blue are 20 Hz and black are 50Hz excitation. **Images are in color.**

Measurement of mechanical properties of active skin

We attempted measurements of the mechanical properties of the active skin. The first method attempted was to measure gross mechanical properties by inflating skin tissue. O-rings were glued onto the skin to maintain their natural tension and to prevent damage during removal from the underlying musculature. The tissues were then mounted in an inflation device and inflated with water to measure the pressure vs volume. The average modulus of the tissue can be obtained by this method. Fig. 2 shows an initial trial conducted with octopus skin. This tissue was freeze-thawed and hence is not representative of live tissue.

We also attempted similar experiments with cuttlefish skin, but we faced several challenges. The first is that when the o-ring was glued to the tissue (Fig. 3A), the skin was taut, but upon removing the tissue, the outer layer of skin shrank significantly (Fig. 3B&C). Presumably the skin was under tension in the live animal and relaxes upon cutting it away. This problem was mitigated by dissecting away much of the connective tissue prior to gluing the o-ring (Fig. 3D). The second was that the skin was heterogeneous in the thickness direction. This is clearly evident from the wrinkles that have formed (Fig. 3C) due to the shrinkage of the tissue: the presence of wrinkles indicates a significant heterogeneity in modulus between the outermost skin layer and the underlying connective tissue. Thirdly, inflation experiments resulted in strongly non-symmetric inflations indicating heterogeneity along the skin direction as well. Accordingly the macroscopic measurements were deemed to be unreliable.

Local mechanical properties were measured by Atomic Force Microscopy (AFM). Glass beads of 15-20 μm diameter were glued onto an AFM cantilever and used to probe the mechanical properties of cuttlefish (*S. officinalis*) skin. The chief interest was in probing whether the mechanical properties of the skin are significantly different in the papilla region as compared to elsewhere. Fig. 4 illustrates the results of scanning across one papilla. While this method seemed promising at first, there were three significant challenges. The first is that the skin of a cuttlefish has an outermost layer of epithelial cells which appear “slimy” to the touch and are highly compliant. This layer is estimated to be 2-4 μm thick – a significant part of the range of AFM indentation. Second, adhesion between the epithelial layer and the AFM probe can obfuscate the measurements. Fig. 4A shows a case in which the cantilever deflection (i.e. the force) did *not* change during the initial approach, and in this case, the point of contact (when the bead attached to the AFM tip first touches the skin) could be obtained reliably. In many cases however, the cantilever deflection was decreasing (i.e. force was reducing) during the initial indentation, possibly indicating adhesion. However the most severe challenge is fundamental: since the cuttlefish skin is “active”, fresh skin remains mobile due to muscular motion. This problem is not expected with other types of biological tissue. Certainly one may resolve this last problem by waiting until the skin has died, but at the cost of making the data less relevant to live animals.

In order to alleviate this problem we developed a new and simple method of immobilizing the skin mechanically. It consisted of metal foil laser-machined in the shape of an annular washer (Fig. 5) with numerous “prongs” to immobilize the skin in a very small region. This method of immobilization was used in some experiments.

We also developed a method of measuring mechanical properties of the skin locally, but with larger indentation than possible with AFM. The chief motivation for this was that the cuttlefish skin is covered with a single layer of epithelial cells and it was suspected that the AFM was probing the properties of this layer than the local properties of the skin. This was accomplished by modifying a commercial large-scale indentation device with a cantilever deflection probe (Fig. 6A). This permitted microgram forces to be measured accurately while permitting indentations of several hundred microns. This permitted an estimate of the modulus (typically 0.8 kPa) of the cuttlefish skin over lengthscales comparable to a single papilla. The results show that – in contrast to our hypothesis that the papillae would have a higher modulus than the surroundings – the difference between the papillae modulus and the surroundings is not very large.

Overall we deem this portion of the project to be unsuccessful. The problem of skin motion is formidable. This is illustrated in Fig. 6C: roughly 27 hours after sacrificing the animal – but leaving the skin in cold ocean water – the skin remains highly active and the force fluctuates considerably. After warming up the skin, the fluctuations cease because of skin death. We are not able to suggest better ways of measuring skin properties if the skin is active.

It must be emphasized that such measurement of skin properties was originally proposed mainly to test the hypothesis that buckling was the mechanism underlying papillae extension. Recent research from the Hanlon lab (see below) suggests that this is only true for the face papillae of *Sepia Apama*. Most other papillae in other species seem to be activated by a purely muscular mechanism. Thus the measurement of mechanical properties is much less relevant.

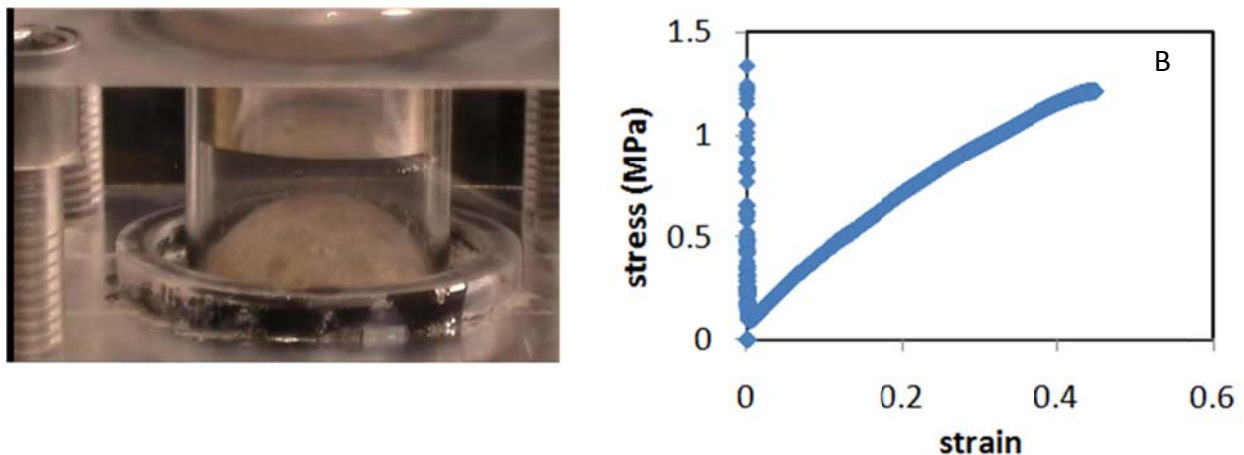


Figure 2: A: Image of octopus skin being inflated by fluid pressure. **B.** Corresponding stress-strain relationship. **Figure is in color.**

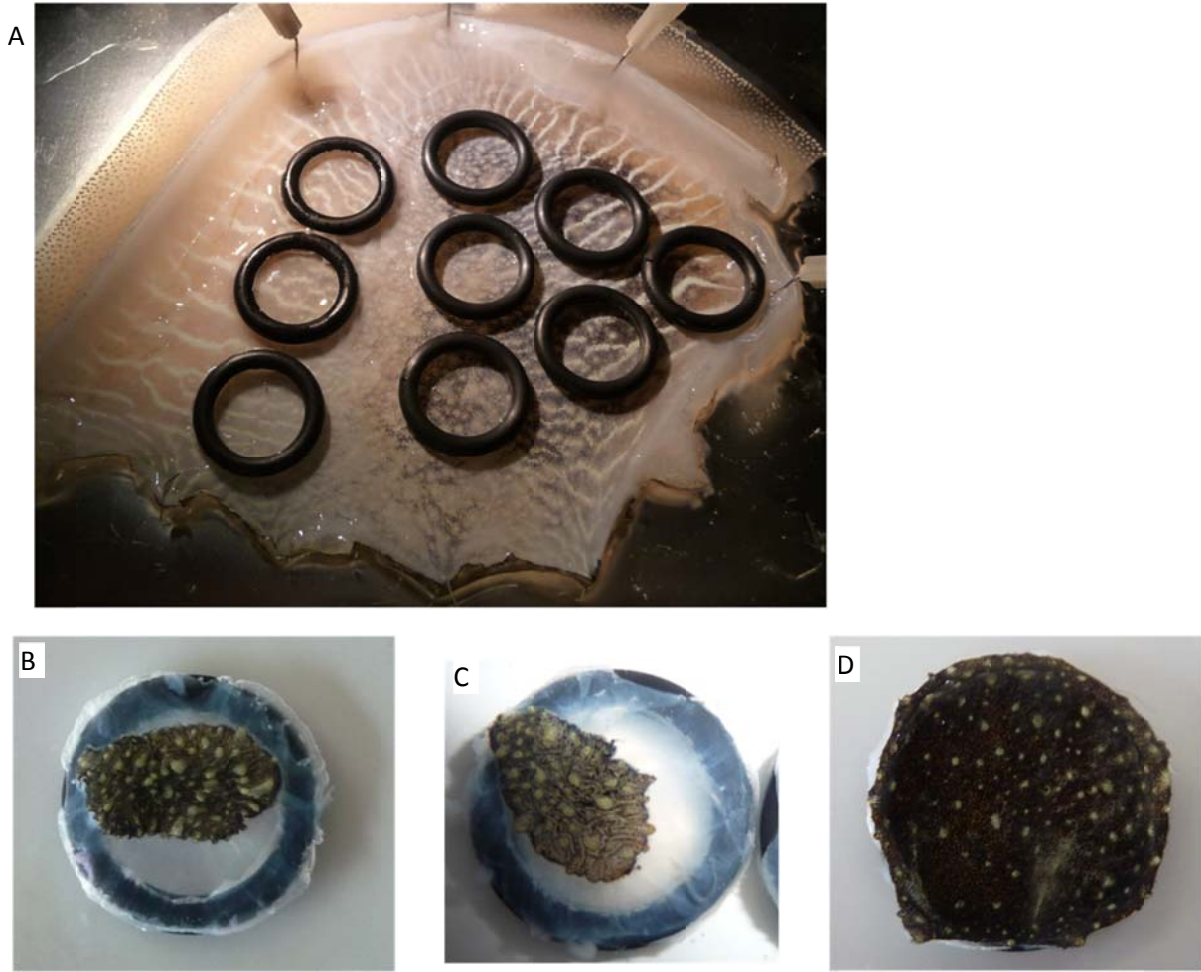


Figure 3: **A.** Cuttlefish (*S. Officinalis*) skin mounted onto o-rings prior to inflation. **B&C.** When the connective is relatively thick, the skin shrinks significantly. Note the wrinkles in **C** which indicate that the outer layer had higher modulus than the lower layers. **D.** Thinner connective tissue. **Figure is in color.**

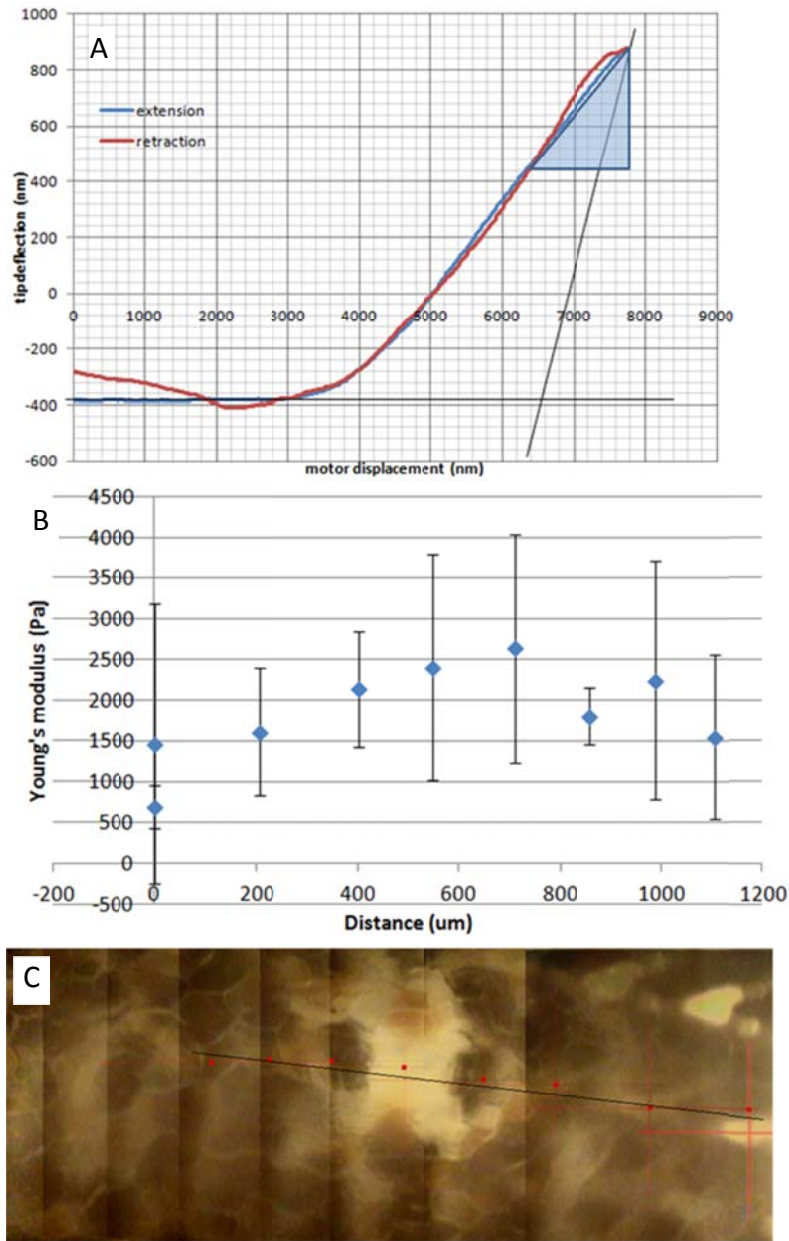


Figure 4: **A.** An example of AFM indentation signal when indenting cuttlefish skin. **B:** Collage of several images recorded by the AFM. Indentation was conducted at each of the red points. **C.** Right: Measured modulus. **Figure is in color.**



Figure 5: A metal skin restraint laser-machined from 0.001" thick foil used to immobilize cuttlefish skin (right) during indentation experiments. **Figure is in color.**

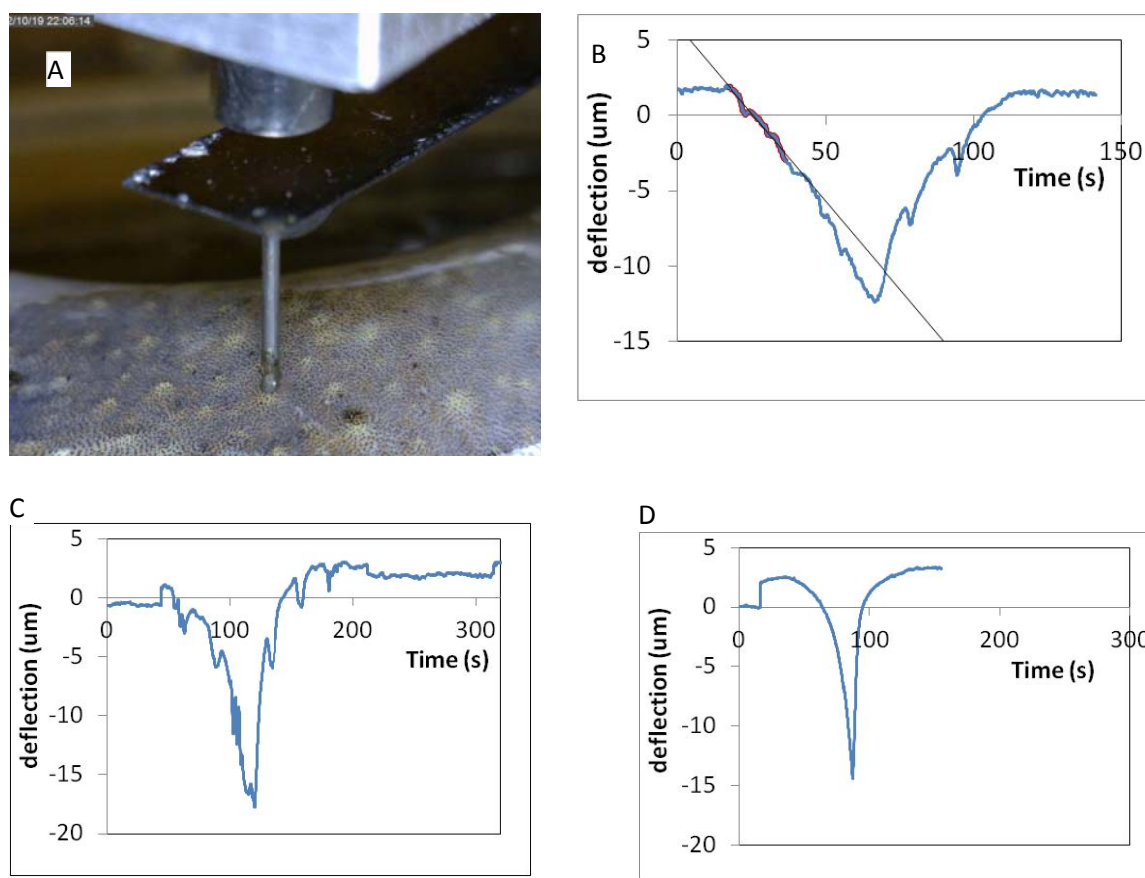


Figure 6: **A.** The cantilever deflection device, using a $\sim 400\ \mu\text{m}$ diameter metal pin as a probe indenting the skin of a cuttlefish. **B.** Force vs deflection data for a indentation-withdrawal experiment. Fitting the initial portion of the data to a straight line, modulus can be extracted. **C&D.** Cantilever deflection signal (proportional to the force) recorded on live skin (**C**, 27 hours after animal death) vs dead skin (**D**, 40 hours after animal death after skin was allowed to warm up). **Figure is in color.**

Morphology of papillae

Finally, the PI has made contributions to ongoing research in the laboratory of Dr. Roger Hanlon on examining the musculature of papillae. Dr. Hanlon's lab was planning a study of a variety of papillae. At the PI's suggestion, Dr. Hanlon extended this research to include the papillae in *Sepia Apama* due to their strong resemblance to buckling skins. Samples were supplied by Australian researchers led by Roger Harcourt, Macquarie University, Sydney. This research showed that most papillae are raised due to action of erector muscles which "squeeze" non-muscular tissue and hence force it to rise away from the skin. The only exception thus far appears to be the face wrinkles of *S. Apama* which have long muscle fibers that induce tissue buckling. A manuscript on this has been submitted by the Hanlon laboratory.

Numerical simulations of buckling phenomena

One hypothesis of this proposal was that skin buckling is a mechanism whereby papillae are expressed. Computational modeling of buckling phenomena are challenging because buckling is an instability, i.e. in a simulation, an unperturbed structure subject to compression will simply deform without buckling. The usual procedure is to first conduct a linear stability analysis of the structure and identify the buckling mode. Then the simulation is repeated with a perturbation at the desired buckling mode, which allows post-buckling behavior to be examined. This approach is difficult to follow for a wide variety of complex problems such as post-buckling mode changes or time dependent phenomena (e.g. with viscoelastic materials or elastic/viscous interactions).

We have developed a numerical method that circumvents these problems. The basic idea is to provide a random perturbation to the structure; upon compression, the deformation grows non-linearly but continuously from the un-buckled to the post-buckled structure. Below we will illustrate this method in several cases, each selected because it is a different type of buckling problem.

- (1) Euler buckling of a cantilever, the most basic example of buckling where the buckling modes are widely separated and hence there is no ambiguity about the mode of buckling (Fig. 7).
- (2) A bilayer laminate buckling where there is a continuum of buckling modes, and the simulation must select the lowest energy mode. (Fig. 8).
- (3) Radial buckling of an annulus where the buckling mode cannot be predicted by linear stability analysis (Fig. 9).

In each of these cases we illustrate that the numerical method gives excellent agreement with either theory or experiments. This simulation approach of applying modulus perturbations is powerful because buckling behavior appears “naturally” without any systematic perturbations needed. Thus pre- and post-buckling behavior can be examined without biasing the structure at any specific buckling mode; furthermore, even complex buckling situations which cannot be predicted by traditional linear stability analysis can be captured. A second advantage of this method is that the perturbation need not be tailored to the geometry. For example, we have shown that even if significant changes are made to the geometry, the exact procedure – even the exact same perturbation field – successfully captures the buckling behavior. Other methods of perturbing the system, e.g. a force or displacement perturbation, would have to be tailored to the new geometry. A manuscript detailing these results had been submitted to *Journal of Applied Mechanics*. The reviewers were positive but suggested that *Journal of Applied Mechanics* is more concerned with fundamental than numerical problems. The manuscript is about to be resubmitted to *Computers and Structures*.

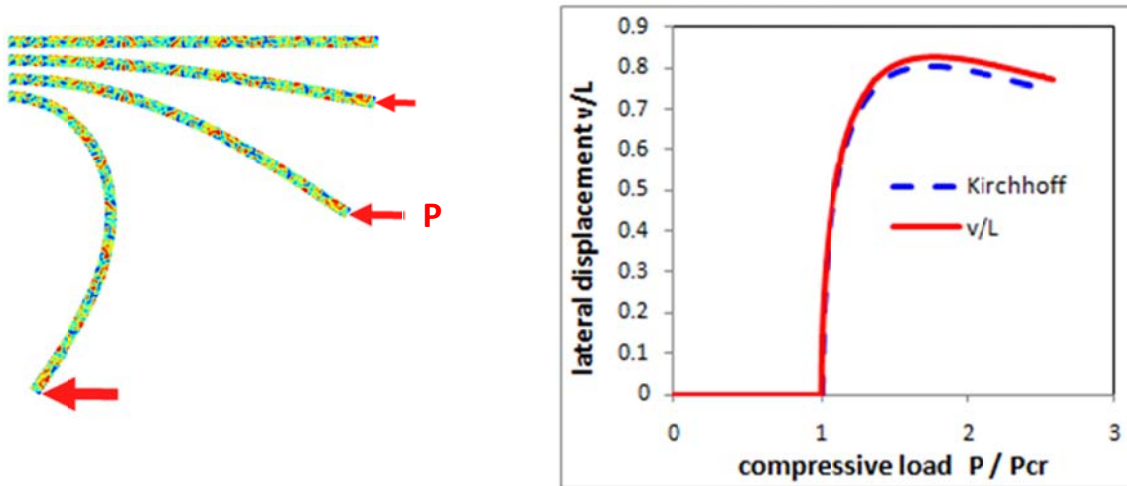


Figure 7: An elastic column cantilevered at its left end is subject to an increasing compressive load P until it buckles. The column is endowed with an elastic modulus that varies randomly (as shown by the color map) with a magnitude of $\pm 1\%$. The left image shows shapes taken by the column as the load is increased. The right shows the vertical displacement of the tip of the column (normalized by its length) as a function of the load P (normalized by the critical buckling load predicted by Euler's equation). The fact that buckling occurs at $P/P_{cr} = 1$ indicates excellent agreement with theory. Furthermore, there is also excellent agreement with the non-linear deformation theory of Kirchhoff. **Figure is in color.**

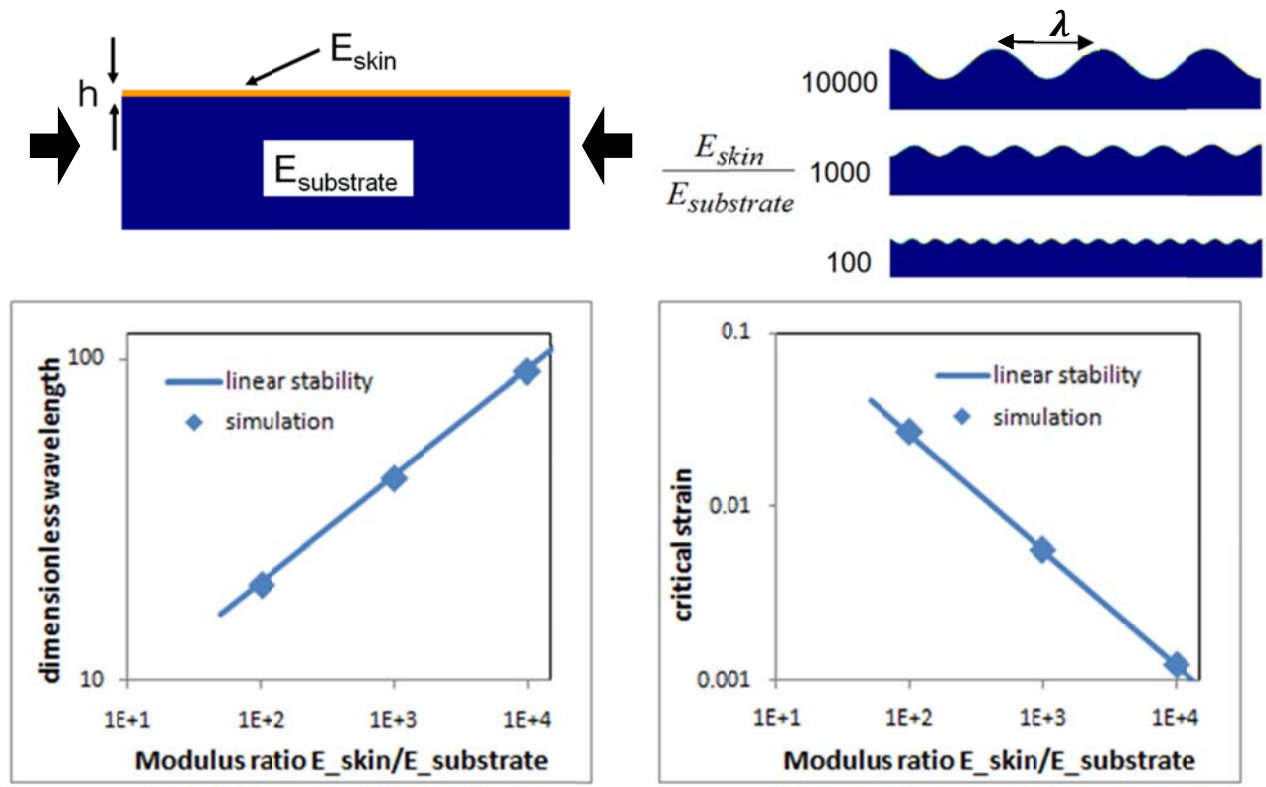


Figure 8: Compression of a stiff skin of thickness h attached to a compliant substrate (geometry indicated top left) undergoes sinusoidal buckling at a wavelength λ that depends on the ratio of the skin modulus to the substrate modulus. Top right image shows simulations at modulus ratios ranging from 100 to 10000. The graphs show the dependence of the normalized wavelength (λ/h) and the critical strain for buckling on the modulus ratio. There is quantitative agreement with linear stability theory[3]. **Figure is in color.**

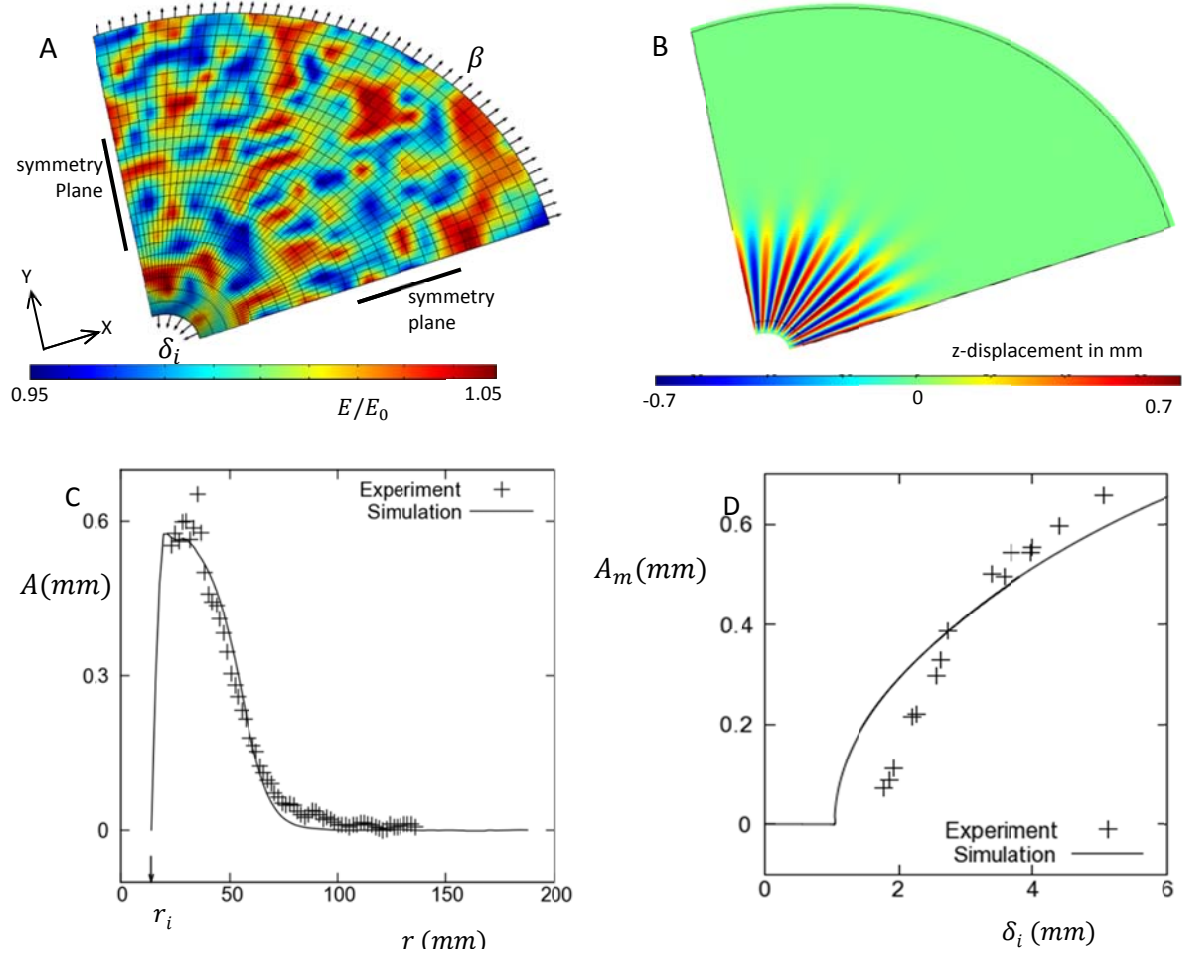


Figure 9: **A:** Geometry and boundary conditions for tension-induced wrinkles on an annular sheet with outer radius $r_o = 185$ mm, inner radius $r_i = 19$ mm, thickness $h = 0.2$ mm. The modulus variation is illustrated by the color map, whereas the thin black lines indicate the FEM mesh. **B:** The vertical displacement field for $\beta = 2.4$ mm and at $\delta_i = 6.19$ mm. Figure is in color in electronic version. Comparison of simulation results against experimental data from Geminard[4]. **C:** Dependence of wrinkle amplitude on radial distance at $\delta_i = 4.9$ mm. **D:** Evolution of maximum wrinkle amplitude with inner displacement δ_i . **Figure is in color.**

Numerical simulations of muscular hydrostats

A muscular hydrostat is a complex muscular structure that deforms at nearly constant volume. Cephalopods are well-known to have numerous muscular hydrostats[5, 6], e.g. squid tentacles, octopus arms, etc. Recent work out of Dr. Hanlon's laboratory has shown that many papillae are actuated by a muscular hydrostat mechanism. Past computational research on muscular hydrostat modeling[7] requires developing dedicated FEM code and numerous input parameters of the musculature are needed. That level of detail is not essential if the goal is simply to estimate shape changes realized by a specific arrangement of muscles, rather than the full dynamics of the process. The goal of our simulation was to develop a facile simulation method, based on commercial software, to do the same.

From a computational point of view, the key challenge for muscular hydrostats is the representation of the complex arrangement of muscles in mathematical form. We sought to do this using the COMSOL Multiphysics software which offers the ability to model thermoelastic deformation of materials, i.e. deformation occurring due to differences in thermal expansion coefficient. Although thermal expansion usually causes volume changes (since expansion occurs uniformly in all directions), by specifying an anisotropic thermal conductivity, volume conservation can be approximated, at least for small deformations.

We considered two typical forms of the anisotropic thermal expansion coefficient to capture the two common muscular arrangements found in animals:

Random in-plane muscle fibers:

$$\alpha = \begin{bmatrix} -\alpha & 0 & 0 \\ 0 & -\alpha & 0 \\ 0 & 0 & 2\alpha \end{bmatrix}$$

Uniaxial muscle fibers:

$$\alpha = \begin{bmatrix} -\alpha & 0 & 0 \\ 0 & \alpha/2 & 0 \\ 0 & 0 & \alpha/2 \end{bmatrix}$$

The overall strategy then was to specify such anisotropic thermal expansion coefficients **locally** within the sample geometry, and then examine the shape changes. Fig. 10 illustrates two cases. The first is of tentacle extension where a shell of annularly-oriented fibers induces contraction (and hence elongation) of a tentacle, whereas the core of axially-oriented fibers induces retraction. The second is a disc of randomly in-plane oriented muscle fibers embedded in a larger disc of inactive material. The shrinkage of this disc then induces a bulge to form – analogous to a papilla.

This approach is ideally-suited to model shape changes due to specific muscular arrangements without needing specialized expertise with FEM: the only input parameters needed are (1) the location and orientation of muscle fibers, and (2) an estimate of the relative moduli of the muscle to the inactive tissue.

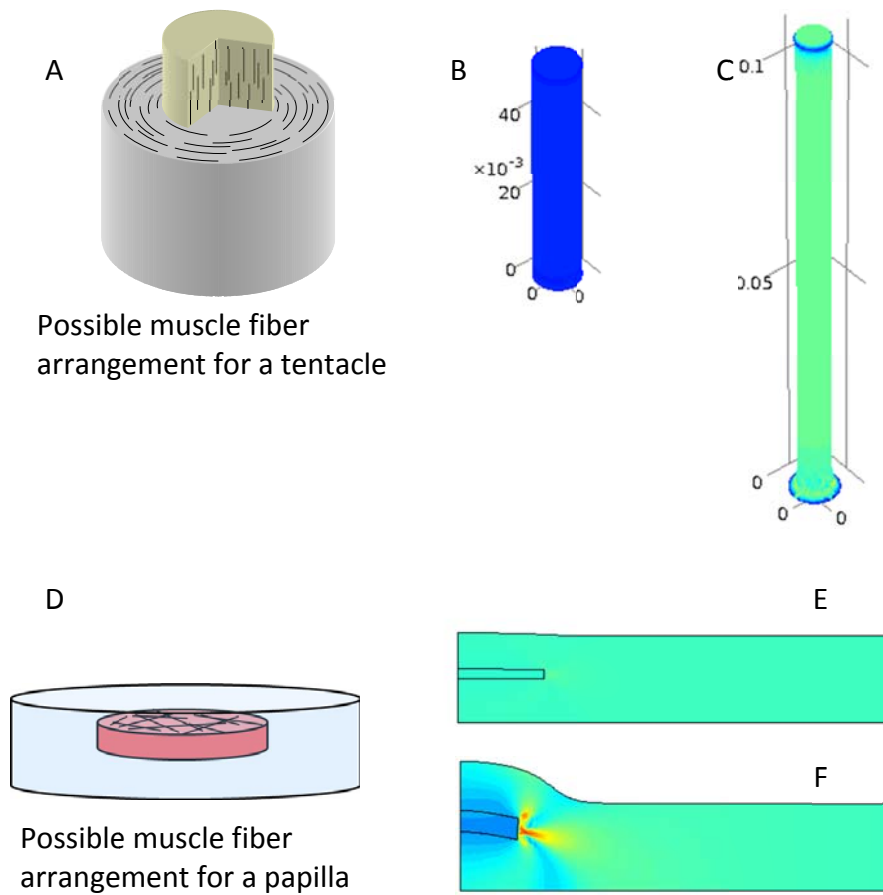


Figure 10: **A:** Muscle arrangement for tentacle extension. **B.** COMSOL model relaxed state. **C.** Shape change after actuating the shell of annular fibers. **D.** Possible muscle arrangement for papilla extension. **E.** Model in relaxed state. **F.** Shape change after actuating the disc to cause radial contraction. **Figure is in color.**

Biomimetic synthetic surfaces with reversible texture

Cuttlefish can express papillae rapidly and reversibly. We sought to achieve similar surface-texturing ability at the “flip of a switch”. We have developed a general platform that can be used to create reversible surface texture with an electrical stimulus. The essential idea (Fig. 11A&B) is to embed shape-memory alloy (SMA) wires into an elastomeric material; upon applying a voltage, the Joule-heating of the wire can induce compression in the elastomer. One can then employ the compressive strain at the surface to drive a buckling transition to achieve rapid and reversible surface texture. There are different ways in which this may be done; one example is to endow the surface with a stiff skin which then buckles. This is analogous to wrinkles developed on our forehead due to muscle-induced compression of the skin. Recent research (see above) from Dr. Hanlon’s lab suggests that wrinkles on the cuttlefish *S. Apama* appear by the same mechanism. Other possible mechanisms include compression-induced delamination as well as compression-induced snap-buckling.

Fig. 11C&D illustrates a practical implementation where a strip of stiff plastic is glued to an elastomer in which a SMA wire is embedded. The location of wrinkles can be changed rapidly by simply actuating different parts of the wire. We have also shown that the timescale of actuation depends on the voltage used to actuate the SMA and can be less than one second.

We have developed a detailed shear lag model of this process. The key insight to recognize is that the wire transfers stress to the elastomer which in turn transfers the stress to the stiff surface. The final result of the theory can be expressed in a simple equation: buckling requires the following criterion to be met:

$$\frac{\epsilon_{SMA}}{\epsilon_c} \frac{L^2}{hH} \frac{G_e}{E_f} > 1$$

where ϵ_{SMA} and ϵ_c are the strain in the SMA wire and the critical strain for buckling the film, L , H , and h are the length of the film, thickness of the elastomer between the wire and the film, and film thickness respectively, and G_e and E_f are the moduli of the elastomer and film respectively.

Thus (1) an elastomer of excessively low modulus will not transfer stress effectively and hence the surface strain will be low but (2) an elastomer of excessively high modulus will resist the SMA deformation more effectively, and hence the strain will reduce. Moreover, since the stress in the strip builds up “from the ends” as typical for all shear lag situations, there is necessarily a region near the ends of the actuation where the compressive stress is too small to induce wrinkles. Thus the smallest region which can wrinkle is limited not just by heat transfer, but also by the fundamental mechanics of stress transfer. This is not just relevant to the present situation, but to any embedded actuator which seeks to induce surface strain.

A manuscript detailing these results has been submitted to *Journal of Intelligent Material Systems and Structures*.

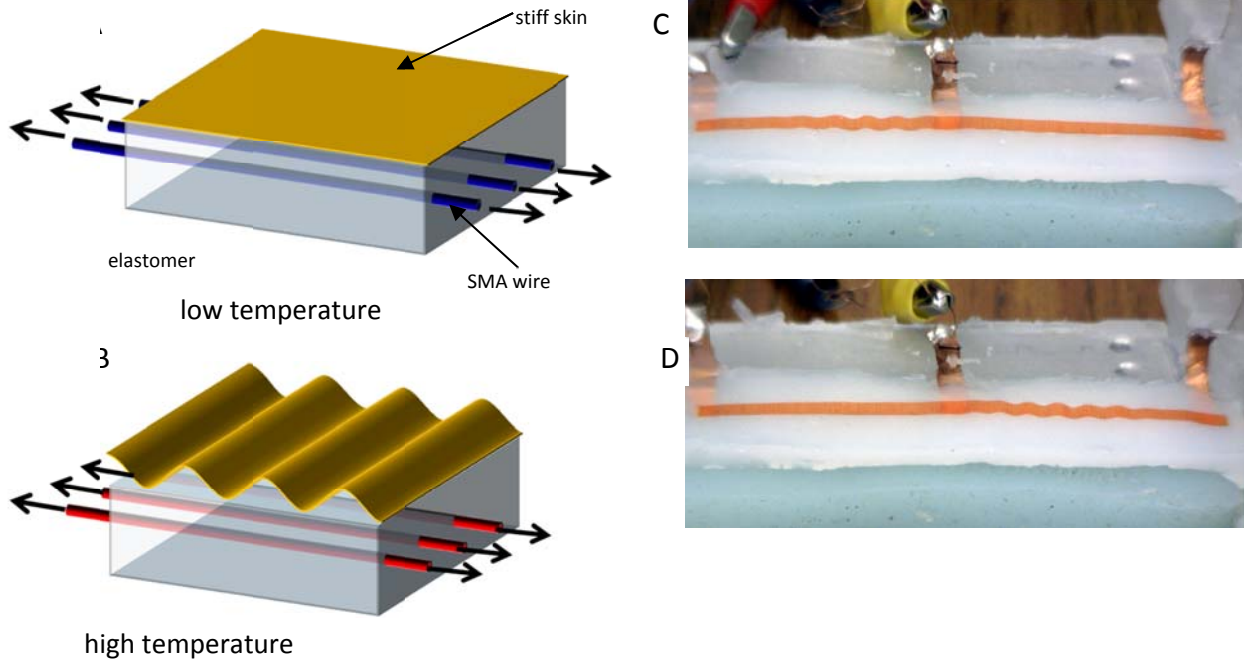


Figure 11: Schematic of SMA-elastomer composites as smart materials. **A:** The SMA wires are at low low temperature and the elastomer is stress-free. **B:** Heating causes shrinkage of the SMA, and hence of the elastomer. The surface compressive strain drives buckling. Arrows indicate an external bias force (e.g. a spring or deadload) that ensures reversibility upon cooling. **C&D.** The location of wrinkles being controlled by changing the region of actuation of an SMA wire embedded in the elastomer. **Figure is in color.**

Other related research

We have conducted research on developing surface texture in two other projects that are related to this AFOSR grant, and these are described here.

Swelling-induced folding of polymer gel films: When a crosslinked polymer film attached to a rigid surface is swollen with solvent, it is in a state of compressive stress and hence susceptible to buckling. Such swelling can lead to the formation of sharp folds by a delamination mechanism[8]. This is of broad interest to morphogenesis in thin films, and is also a potentially facile route to developing high-aspect ratio texture on surfaces. We have discovered that folding greatly promotes spreading, i.e. drops placed on a film spread much more if the film folds than if it does not. We have quantified the effect of various parameters on the folding process and mapped the various morphologies evident due to folding. The results appear to be captured by simple geometric criteria. The results of this research have been submitted to *European Physical Journal E*.

Buckling of elastic films on viscous substrates: When a solid film floating on a liquid is compressed, it buckles[9]. The effect of dissipation effects on this process are not well-understood. Specifically, if the liquid has a high viscosity, mechanical equilibrium is difficult to reach and the *rate* of compression may be expected to play a role. We have examined this issue theoretically and experimentally. Fig. 13 shows an example where a film floating on a highly viscous polymeric liquid is compressed to show wrinkles. These wrinkles have a wavelength far smaller than expected from a balance between gravity and bending energy[9]. Furthermore, the wavelength depends on compression rate, i.e. viscosity plays a major role in this process.

In collaboration with Prof. Rui Huang, U. Texas Austin, we have developed a shear lag model of this process. Briefly, the in-plane displacement of the film, u , can be described by the diffusion equation

$$\frac{\partial u}{\partial t} = \frac{EhH_0}{\eta} \frac{\partial^2 u}{\partial x^2} + \dot{\epsilon}x$$

where h and H_0 are the thickness of the solid film and the liquid layer respectively, η is the viscosity, E is the film modulus, and $\dot{\epsilon}$ is the compression rate. Solving this equation predicts the evolution compressive stress in the film and the qualitative dependence of the wrinkle wavelength on the compression rate and liquid layer thickness. It is also able to explain why there is a wrinkle-free zone at the ends of the film,. We have also conducted a linear stability analysis of this situation to predict quantitatively the dependence of wavelength on these properties. Two manuscripts, one on the experimental results and one on the analysis, are in progress.

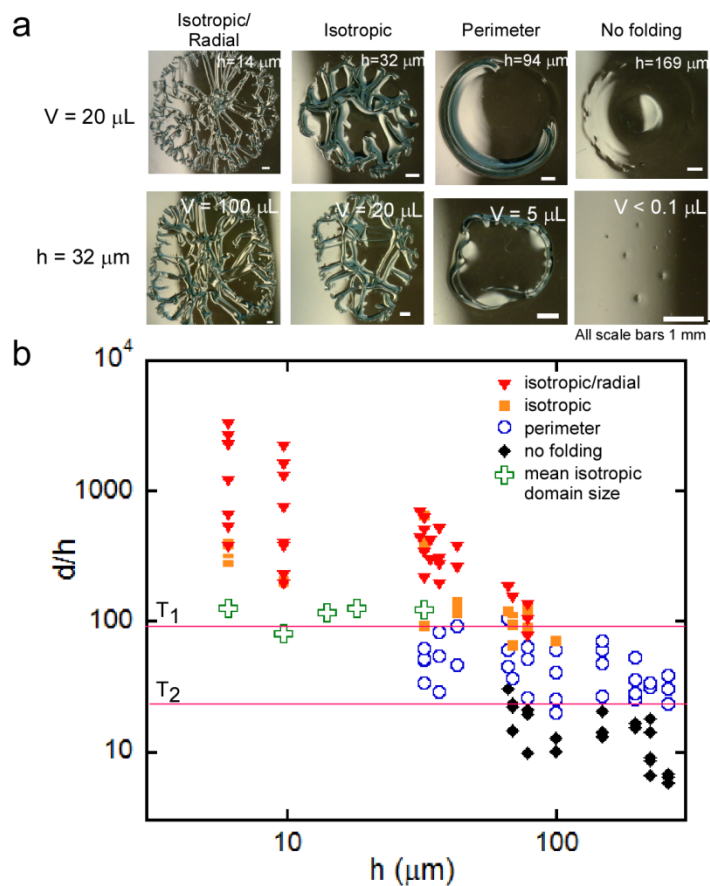


Figure 12: **a:** A drop of toluene placed on a film of PDMS causes delamination and folding. Depending on the size of the drops and film thickness, a variety of patterns ranging from corrals to radially-propagated folds appear. **b:** A morphological map which shows the dependence of the morphology on the film thickness and aspect ratio (i.e. ratio of drop footprint diameter to the film thickness). The transitions appear at approximately fixed values of aspect ratio. **Figure is in color.**

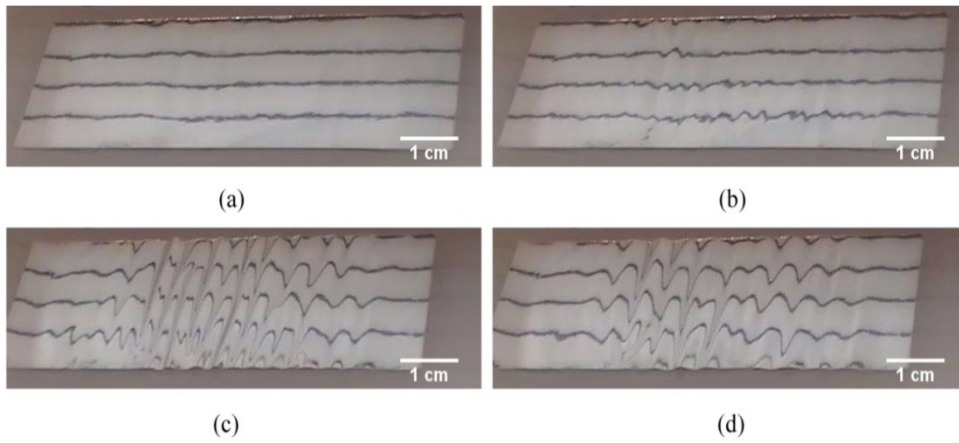
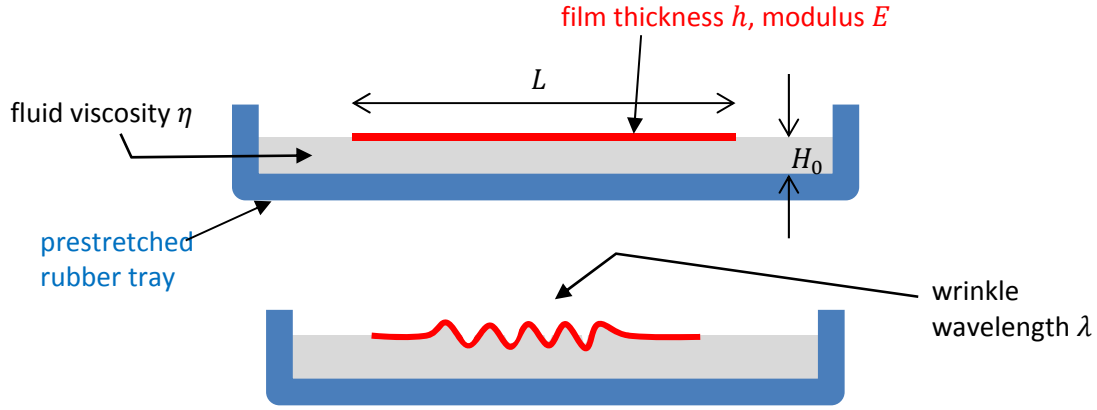


Figure 13: Top: Schematic of experiment: A solid film floats on a high viscosity liquid poured in a pre-stretched elastomeric tray. When the pre-stretch is removed at a specified speed, the viscous stress generated in the fluid layer compresses the film and induces buckling. **a.** Image of a $12.7\ \mu\text{m}$ film floating on viscous polyisoprene. **b&c:** Development of wrinkles, **d.** relaxation upon cessation of compression. **Figure is in color.**

References

1. Hanlon, R., *Cephalopod dynamic camouflage*. Current Biology, 2007. **17**(11): p. R400-R404.
2. Hanlon, R.T. and J.B. Messenger, *Cephalopod Behaviour*. 1998 Cambridge: Cambridge University Press.
3. Jiang, H.Q., et al., *Finite deformation mechanics in buckled thin films on compliant supports*. Proceedings of the National Academy of Sciences of the United States of America, 2007. **104**(40): p. 15607-15612.
4. Géminard, J.-C., R. Bernal, and F. Melo, *Wrinkle formations in axi-symmetrically stretched membranes*. The European Physical Journal E: Soft Matter and Biological Physics, 2004. **15**: p. 117-126.
5. Kier, W.M. and A.M. Smith, *The morphology and mechanics of octopus suckers*. Biological Bulletin, 1990. **178**(2): p. 126-136.
6. Kier, W.M. and K.K. Smith, *Tongues, tentacles and trunks - The biomechanics of movement in muscular-hydrostats*. Zoological Journal of the Linnean Society, 1985. **83**(4): p. 307-324.
7. Liang, Y., R.M. McMeeking, and A.G. Evans, *A finite element simulation scheme for biological muscular hydrostats*. Journal of Theoretical Biology, 2006. **242**(1): p. 142-150.
8. Velankar, S.S., V. Lai, and R.A. Vaia, *Swelling-induced delamination causes folding of surface-tethered polymer gels*. Acs Applied Materials & Interfaces, 2012. **4**(1): p. 24-9.
9. Pocivavsek, L., et al., *Stress and fold localization in thin elastic membranes*. Science, 2008. **320**(5878): p. 912-916.